

# Langmuir–Blodgett multilayers of native and synthetic glycerol–dialkyl–glycerol tetraether derivatives from archaea

T.S. Berzina <sup>a,1</sup>, V.I. Troitsky <sup>a,1</sup>, S. Vakula <sup>b</sup>, A. Riccio <sup>c</sup>, A. Gambacorta <sup>c</sup>, M. De Rosa <sup>c</sup>,  
L. Gobbi <sup>d</sup>, F. Rustichelli <sup>d</sup>, V.V. Erokhin <sup>a,c</sup>, C. Nicolini <sup>e</sup>

<sup>a</sup> *Technobiochip, Marciana, Livorno, Italy*

<sup>b</sup> *EL.B.A. Foundation, Portoferraio (LI), Italy*

<sup>c</sup> *Istituto di Biochimica delle Macromolecole, II University of Naples, and ICMIB, Naples, Italy*

<sup>d</sup> *Istituto di Scienze Fisiche, University of Ancona, Ancona, Italy*

<sup>e</sup> *Istituto di Biofisica, University of Genoa, Genoa, Italy*

Received 11 October 1994; in revised form 10 April 1995

## Abstract

Langmuir–Blodgett films of monosubstituted glycerol–dialkyl–glycerol tetraether with phosphomyoinositol group extracted from thermophilic archaeobacterium *Sulfolobus solfataricus* are successfully deposited. However, the procedure of film deposition is rather complicated. Reproducibility of the results is not satisfactory. Non-uniform areas are often observed in the films despite the fact that the same optimum conditions of deposition are used. The films do not possess stability in water. To overcome these problems a series of semisynthetic archaeol lipids have been synthesized. The monosuccinylated and disuccinylated glycerol–dialkyl–glycerol tetraethers appeared to be the most promising compounds. Highly uniform films of barium salt of these lipids can be deposited by the Langmuir–Blodgett technique. The multilayers are stable in aqueous solutions. The quality of deposition of disuccinylated tetraether is similar to that of the usual fatty acid salts. The films are studied by optical microscopy, transmission electron microscopy, X-ray small-angle diffraction, and electron diffraction techniques. Contact angles for the deposited films are measured as well. Data obtained from the surface pressure–area isotherms, X-ray diffraction, and contact angle measurements show that the U-shape of molecules is preferred rather than the extended form.

**Keywords:** Air–water interface; Archeon lipid; Glycerol–dialkyl–glycerol tetraether; Carboxyl group; U-shaped conformation; Langmuir–Blodgett

## 1. Introduction

Archaea is the third evolution line of life in addition to Eubacteria and Eukaria [1]. It comprises a variety of extremophilic bacteria living in severe conditions, i.e. at high temperatures, extreme pH values, or in saturated solutions. Unusual structural features of the archaeol lipids [2] play an important role in the membrane stabilization. These are bipolar lipids with ether linkage of isoprenoid chains to some polyols. For example, membrane lipids of thermophilic archaeobacteria *Sulfolobus solfataricus*, growing optimally at 87 °C and pH 3, are composed of two polar heads linked with each other by two hydrophobic isoprenoid chains  $C_{40}H_{72-80}$ , which are practically twice as long as the chains of the usual membrane lipids.

Owing to such properties bipolar archaeol lipids are promising materials for the creation of artificial media stable at extreme conditions just destined by nature for incorporation of some functional molecules, for example, proteins. The structure and polymorphism of a variety of lipids extracted from *S. solfataricus* have been investigated by the X-ray scattering technique [3,4] to determine the origin of their thermal stability. One problem of great interest is to develop technological methods to produce highly organized structures on the basis of such archaeol lipids.

The possible way to solve this problem is the application of the Langmuir–Blodgett (LB) technique [5,6] for depositing thin films of lipids from archaea. The LB technique enables one to create systems of complex structure where monolayers of different types of molecules possessing various properties are arranged in the required order across the thickness of the film, i.e. to accomplish “construction” at the molecular level [7]. One can also embed different biological

<sup>1</sup> Permanent address: Zelenograd Research Institute for Physical Problems, Moscow, Russia.



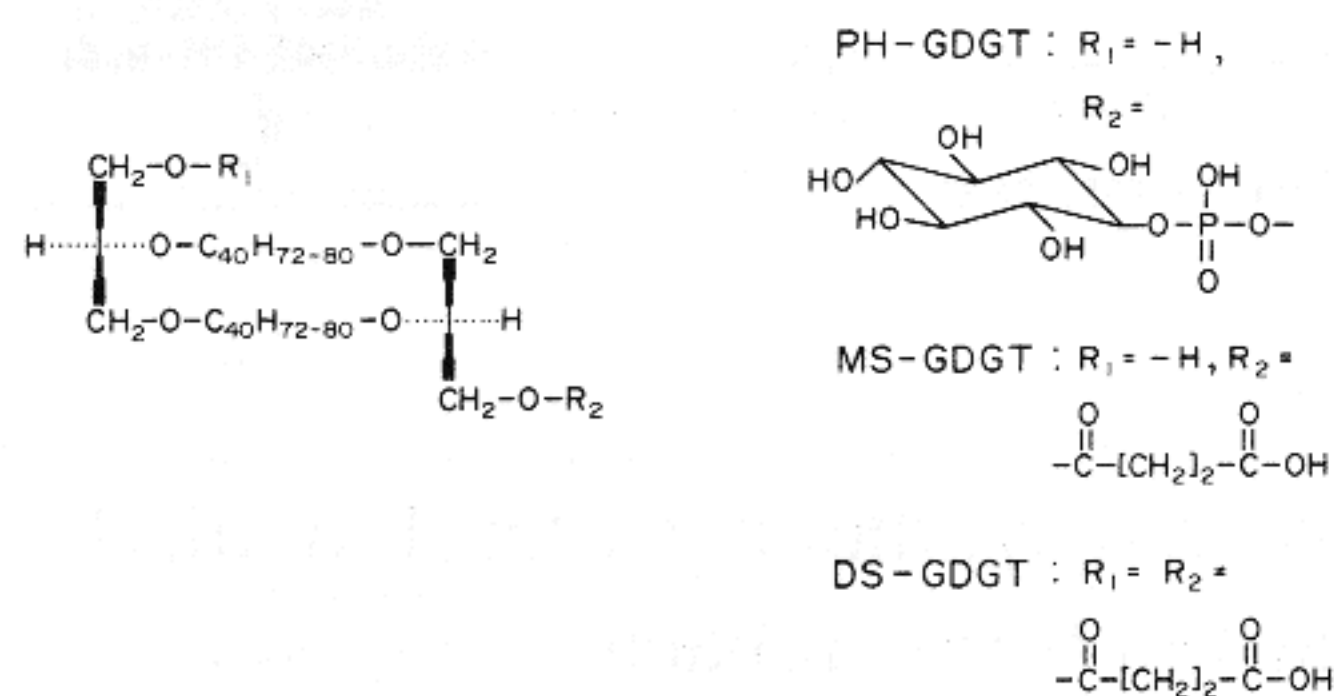


Fig. 1. Formulae of the native lipid PH-GDGT and synthetic derivatives MS-GDGT and DS-GDGT.

molecules into the monolayers or adsorb them on the latter to produce biologically active systems [8]. However, lipids from archaea are unusual compounds for the LB method because of their bipolar structure.

Langmuir monolayers of some native and semisynthetic lipids from *S. solfataricus* have been studied by Rolandi et al. [9]. In particular, they found that the hydrolysed lipid GDGT, i.e. non-substituted glycerol-dialkyl-glycerol tetraether, forms unstable monolayers. Bipolar lipids of methanogenic archaeobacterium *Methanospirillum hungatei* have been investigated at the air-water interface by Tomoia-Cotisel et al. [10]. The U-shaped hydrocarbon chain conformation appears to be preferred to an extended chain form for these lipids. Dote et al. [11] studied the properties of the monolayers of two bipolar tetraethers produced from the lipids of thermoacidophilic archaeon. They did not find essential evidence for the U-shaped molecules and suppose that an extended form is more likely. It should be noted that the results of various authors on the study of the monolayers of similar archaeol lipids sometimes differ strongly. That may be caused by the difference of particular methods of lipid extraction or monolayer preparation. In such a situation one can meet unpredictable difficulties when depositing the LB films.

The present work is the second part of a series of papers with the common task to create thin LB films on the basis of archaeol lipids containing valinomycin molecules which are able to interact selectively with potassium ions. In the first paper we reported on the deposition and study of the LB films of three native lipids. Here we deposited first the LB films of another native lipid, monosubstituted glycerol-dialkyl-glycerol tetraether with phosphatidyl group (PH-GDGT), extracted from *S. solfataricus* (Fig. 1). However, electron microscopy images of the deposited multilayers often show some non-uniform areas. Precipitated crystalline aggregates are also observed under any conditions of deposition. Moreover, the films of PH-GDGT as well as the films of other native lipids deposited before do not possess stability in aqueous solutions, which is quite necessary for a sensitive system for the detection of potassium ions. To solve these problems new archaeol lipids with modified head groups have been synthesized. In particular, starting from GDGT we have

obtained the monosuccinylated (MS-GDGT) and disuccinylated (DS-GDGT) glycerol-dialkyl-glycerol tetraethers (Fig. 1). Uniform LB films with morphology similar to that of fatty acid salts have been obtained for these two compounds, but reproducibility of the results is considerably better with DS-GDGT than MS-GDGT. In the third part of this series of works the results on the deposition and study of LB films of alternating valinomycin and DS-GDGT barium salt bilayers are reported.

## 2. Experimental details

Procedures of isolation and purification of the lipid PH-GDGT are described in detail elsewhere [12]. The hydrolysed lipid GDGT was produced as reported by De Rosa et al. [13]. The GDGT was the initial component for the synthesis of the lipids MS-GDGT and DS-GDGT.

Synthesis of the MS-GDGT was carried out as follows. Succinic anhydride (12.7 mg) was added to the solution of GDGT in pyridine (47 mg in 1.5 ml). The mixture was stirred at room temperature for 12 h. The reaction was monitored by thin-layer chromatography (TLC) on 0.25 mm layer of silica gel 60 F<sub>254</sub> Merck ( $R_F$  0.7 for GDGT in chloroform). Upon completion of the reaction, 5 ml of methanol were added and the mixture was stirred for few minutes. The mixture was acidified with 10 ml of aqueous 0.1 N HCl and extracted with four portions of ethyl ether. The extract was washed with water until neutral and dried under reduced pressure. The product was purified by chromatography on a silica gel column (70–230 mesh ASTM, Merck 30 × 2 cm) with chloroform-methanol mixture (9:1 v/v) as eluent, and dried in vacuo, yielding 12 mg (24%) of the product. It showed one spot with  $R_F$  0.63 in the solvent system chloroform-methanol (9:1 v/v). Two signals of methine carbons of glycerol and succinylated glycerol at 78.40 and 76.54 ppm as well as two signals of C-1 *sn* carbons of the primary hydroxyl group and the esterified one of the glycerol moieties respectively at 63.34 and 62.96 ppm appear in the <sup>13</sup>C-NMR spectrum.

To synthesize the DS-GDGT lipid succinic anhydride (654 mg) was added to the solution of GDGT in pyridine (170 mg in 5 ml). The mixture was stirred at room temperature for 12 h and the reaction was monitored by TLC on a 0.25 mm layer of silica gel 60 F<sub>254</sub>, Merck ( $R_F$  0.7 for GDGT in chloroform). The mixture was acidified with 20 ml of aqueous 0.05 N HCl and extracted with three portions of ethyl ether. The extract was washed with water until neutral and dried under reduced pressure. The product was purified by chromatography on a silica gel RP 18 column (Lobar, Merck 30 × 1.5 cm) with chloroform-methanol mixture (1:1 v/v) as eluent and dried in vacuo yielding 68 mg (35%). It showed one spot with  $R_F$  0.30 on TLC in the solvent system chloroform-methanol (9:1 v/v). The <sup>13</sup>C-NMR spectrum shows one signal of methine carbons at 76.48 ppm and one signal of C-1 *sn* carbons at 64.44 ppm.



The LB-MDT System (MDT, Moscow) was used for recording surface pressure–area isotherms and deposition of the LB films for X-ray, electron diffraction, and electron microscopy studies. LB films for contact angle measurements were deposited with a KSV 5000 System. The quality of all deposited films was checked with an AXIOSCOP (Carl Zeiss) optical microscope at magnifications up to 1000. Transmission electron micrographs and electron diffraction patterns were obtained with a CM 12 (Philips) electron microscope at an accelerating voltage of 80 kV. X-ray small-angle diffraction curves were recorded with an AMUR-K diffractometer (Institute of Crystallography, Moscow) using a position-sensitive detector and Cu K $\alpha$  non-filtered radiation ( $\lambda = 0.154$  nm). Contact angle measurements for the deposited films were carried out as proposed by Ulman [14]. Water for subphase preparation was distilled with an AQUATRON A4S distillator and deionized with the UHQ-II ELGASTAT System. Resistivity of water was equal to at least  $10^{18}$  M $\Omega$  cm.

Silicon and sapphire substrates were used during development of the deposition method to check the possibility of film formation on surfaces of different types. To obtain hydrophilic surfaces the substrates were treated by sulphuric acid or by air glow discharge. Hydrophobic silicon substrates were obtained by treatment with dimethyldichlorosilane or concentrated hydrofluoric acid. In the case of treatment with hydrofluoric acid the substrates were used for deposition immediately after removal of silicon oxide. From 19 to 60 monolayers were deposited for observation with the optical microscope. Films of 10–90 monolayers were deposited onto hydrophobic silicon substrates for X-ray diffraction measurements. Fifteen monolayers of each compound were transferred onto copper grids covered by collodion films 10–20 nm thick for electron microscopy and electron diffraction studies. For contact angle measurements the films of PH-GDGT, MS-GDGT and DS-GDGT consisting of 10–40 monolayers deposited onto hydrophobic silicon substrates under optimum conditions presented below were used. In addition, the films of DS-GDGT (80–180 monolayers) deposited by LB or horizontal lifting techniques from  $10^{-4}$  M barium acetate solution at pH from 2 to 11 were studied.

Trials of PH-GDGT film deposition were performed under various conditions, but the best results were obtained as follows. An initial solution of the compound in chloroform–methanol–water mixture (65:25:4 by vol.,  $2.9$  mg ml $^{-1}$ ) was diluted by chloroform–ethanol–hexane (1:2:3 by vol.). The final concentration of the PH-GDGT solution was  $0.33$  mg ml $^{-1}$ . The films were deposited by the horizontal lifting technique from the surface of pure water after compression of the monolayer up to  $25$  mN m $^{-1}$ . Deposition by the LB technique was carried out at the same surface pressure and at pH 5.0 with a speed of  $0.25$  cm min $^{-1}$ . Pause duration for substrate drying in the upper position was 3 min. In the case of deposition by the LB technique the substrates covered by four monolayers of barium behenate were used. Spreading of the compounds MS-GDGT and DS-GDGT at the air–water inter-

face was performed using the solution in chloroform–hexane mixture (1:2 v/v) with concentrations of  $0.33$  and  $0.23$  mg ml $^{-1}$  respectively. The water subphase contained  $10^{-4}$  M of barium acetate at pH 7.0. The films were deposited with a speed of  $0.5$  mm min $^{-1}$  by the LB technique at surface pressure values of  $22$  and  $26$  mN m $^{-1}$  for the MS-GDGT and DS-GDGT respectively. The pause duration for film drying after deposition of each bilayer was 2 min.

The film stability in pure water was checked in each case. If no recrystallization or removal of the film from the substrate took place during 1–2 h the same trials were repeated with water solutions of sodium and potassium ions at the concentration of  $10^{-3}$  M for several pH values in the range 3–9. To detect film morphology deterioration we observed the multilayers 50–100 nm thick deposited onto silicon substrates with the optical microscope before and after immersing them in water solution. Such films on silicon surface possess intense interference colour which changes strongly with the variation of the thickness. Thus, variations of thickness of about 3–5 nm can be detected easily. To avoid contamination of the films with components of the solutions used the samples were always washed quickly in pure water and droplets of water were removed with a stream of compressed air.

### 3. Results and discussion

#### 3.1. Experimental data on the deposition, structure and morphology of PH-GDGT films

First of all, multilayers of the native lipid PH-GDGT were deposited. That was of interest because some structural parameters of the films could be compared with the data obtained for bulk material [4]. The surface pressure–area isotherm (Fig. 2) shows the area per molecule extrapolated to zero surface pressure of  $0.99 \pm 0.03$  nm $^2$ . Y-type deposition takes place. The best average transfer ratio of 0.8 was achieved when the deposition was onto hydrophobic substrates. Prac-

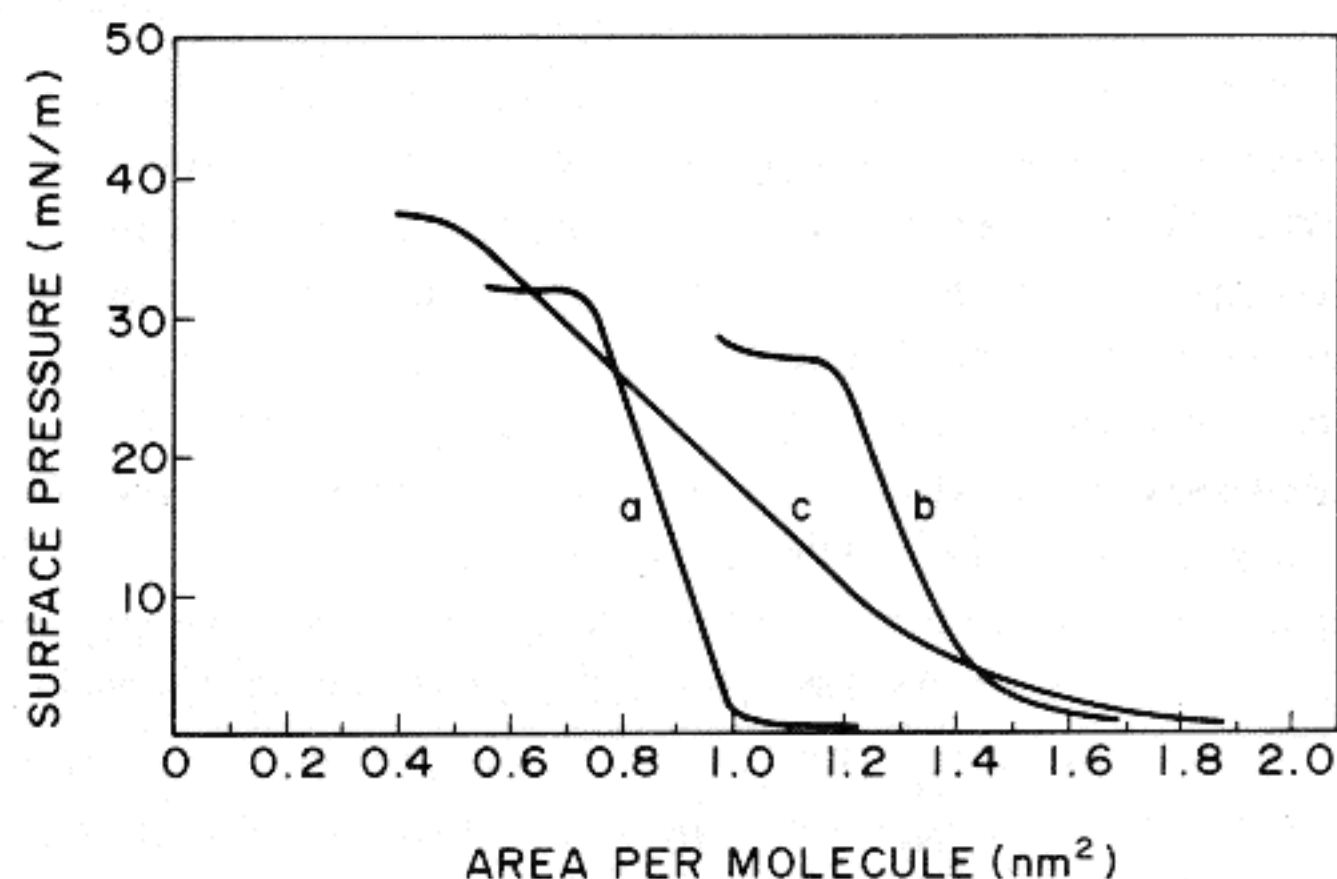


Fig. 2. Surface pressure–area isotherms of PH-GDGT (a), MS-GDGT (b) and DS-GDGT (c) monolayers spread at the surface of pure water. Areas per molecule extrapolated to zero surface pressure are equal to  $0.99$ ,  $1.45$ , and  $1.47$  nm $^2$  for curves (a), (b) and (c) respectively.



tically no transfer takes place when depositing onto hydrophilic substrates. However, non-uniform areas in the form of strips are always observed for the best films also. Such behaviour is typical when the adhesion of the film to the substrate is insufficient. To increase the adhesion the substrates were covered before the deposition of PH-GDGT films by four monolayers of barium behenate. In this case the average transfer ratio increases up to 0.95. The X-ray diffraction curve contains only one Bragg peak corresponding to the period of  $4.8 \pm 0.1$  nm (Table 1).

Actually, the above reported area per molecule can be slightly larger. Indeed, optical and electron microscopy studies of the films deposited under different conditions show bulk precipitates like those which arise in usual LB films when the problems of spreading are not completely solved. Insufficient spreading seems to be a reason for their origin also because the shape and content of these precipitates do not practically depend on the conditions of monolayer compression and film deposition. An example of film morphology is presented in Fig. 3(a). We can expect that the real area per molecule is a little more than  $1 \text{ nm}^2$ .

The film possesses a poor order in the layer plane which follows from the electron diffraction pattern also shown in Fig. 3(a). Point-like reflections from the precipitated crystallites mentioned above can be observed in the same diffraction pattern.

### 3.2. Structure of PH-GDGT molecules in a monolayer at the air–water interface

These experimental data seem to show the structure of LB films to be different from that of lamellar phases in bulk specimens in which unsubstituted head groups, i.e.  $-\text{OH}$  ones, are located preferentially in the hydrocarbon region [4]. To

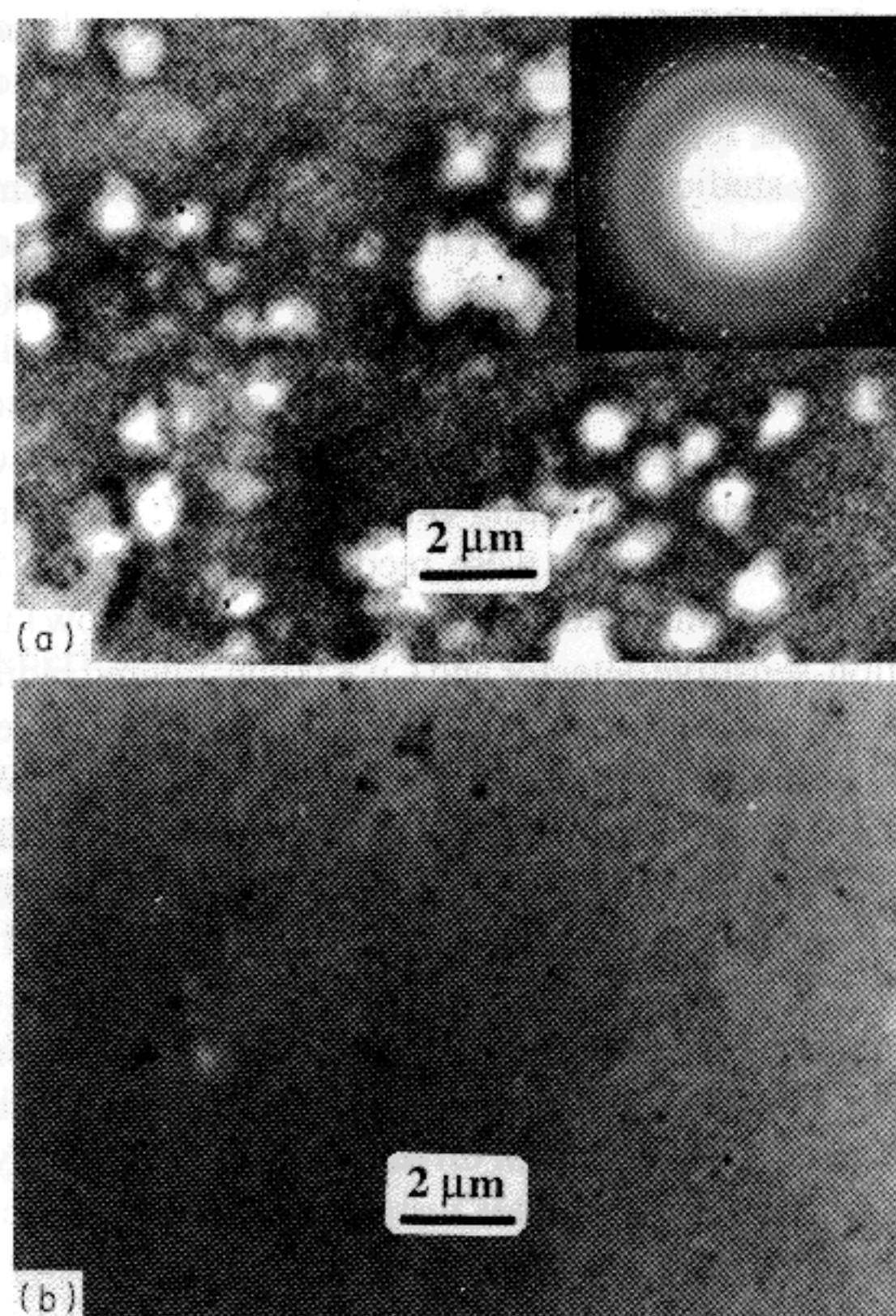


Fig. 3. Transmission electron micrographs of 15 monolayers of PH-GDGT deposited from the surface of pure water at  $23 \text{ mN m}^{-1}$  by the horizontal lifting technique (a) and 15 monolayers of DS-GDGT deposited from the surface of  $10^{-4} \text{ M}$  barium acetate solution at  $26 \text{ mN m}^{-1}$  and pH 7.0 by the LB technique.

substantiate that let us first consider possible variants of molecule arrangement in the monolayer at the air–water interface. If unsatisfactory spreading of the compound is taken into account the area per molecule in a condensed state after

Table 1

X-ray small-angle diffraction data and transfer ratios for LB films of archaeol lipids deposited by the LB technique onto hydrophobic silicon substrates

Lipid	Conditions of deposition		Number of monolayers	X-ray data					
	Subphase	Surface pressure (mN m <sup>-1</sup> )		Peak position (2θ, deg.)	Intensity (arbitrary units)	FWHM (deg.)	Spacing (nm)		
PH-GDGT	pH 5.0	25.0	38	1.82	0.53	0.22	4.80		
MS-GDGT	pH 7.0 10 <sup>-4</sup> M Ba <sup>2+</sup>	22.0	90	2.04	0.15	0.32	4.40		
				4.10	0.05	0.45			
				~1.2	?	?	?		
DS-GDGT	pH 7.0 10 <sup>-4</sup> M Ba <sup>2+</sup>	26.0	60	2.23	1.00	0.26	3.97		
				4.50	0.16	0.24			
Average transfer ratios (numbers of monolayers from N <sub>1</sub> to N <sub>2</sub> )									
N <sub>1</sub>	1	11	21	31	41	51	61	71	81
N <sub>2</sub>	10	20	30	40	50	60	70	80	90
PH-GDGT	0.92	0.98	0.80	0.72					
MS-GDGT	0.60	0.99	1.01	0.95	0.66	0.34	0.45	0.50	0.28
DS-GTGT	1.25	1.02	1.00	0.99	0.99	0.98			



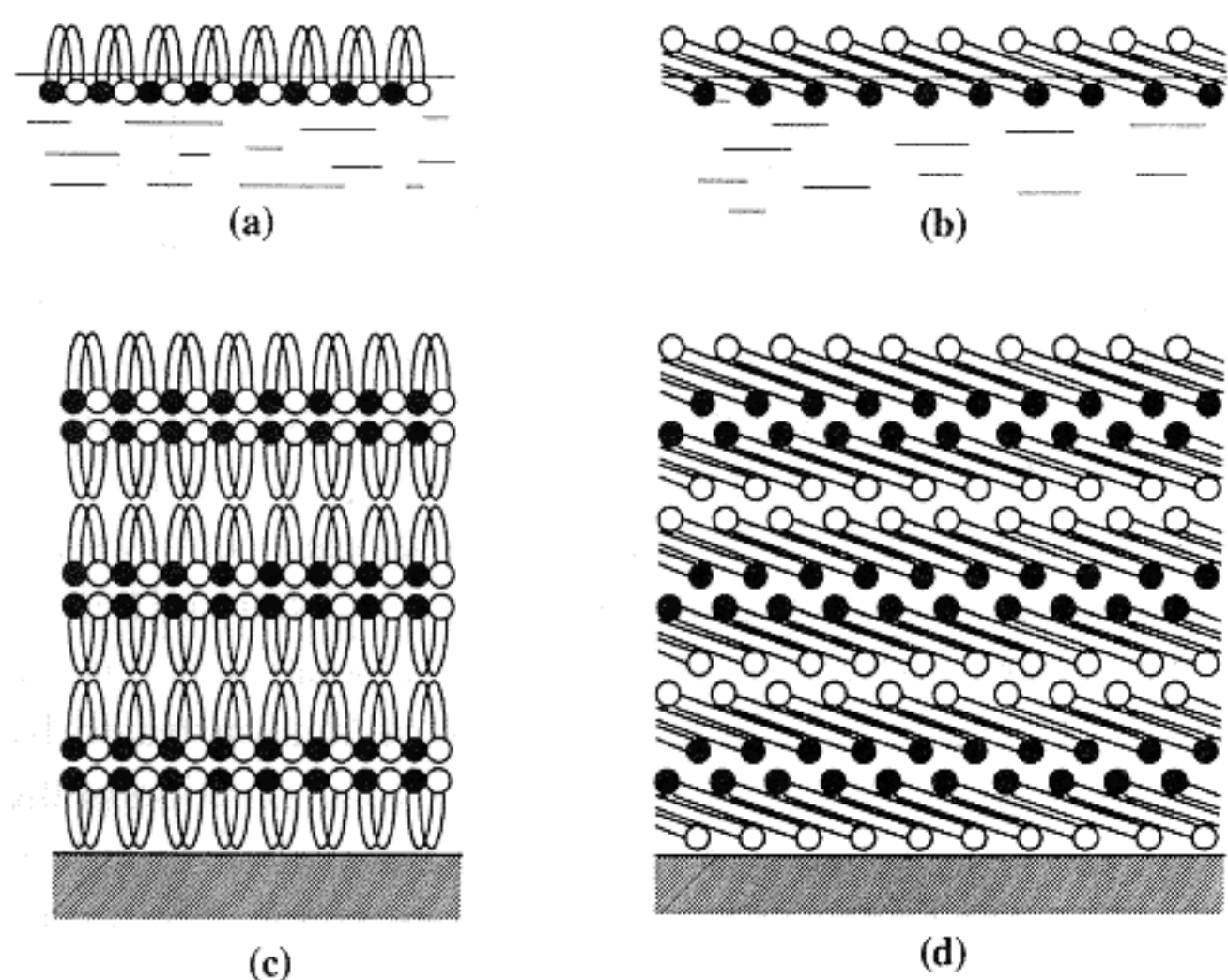


Fig. 4. Probable models of the molecular packing in the PH-GDGT monolayers and multilayers. Monolayer at the air–water interface composed of the molecules in a U-shape (a) and in an extended form (b). Multilayer on the solid substrate composed of the molecules with U-shaped (c) and extended (d) configurations.

extrapolation to zero surface pressure corresponds to the cross-section of four isopranyl chains with the orientation normal to the layer plane because the cross-section of one chain is equal to approximately  $0.27 \text{ nm}^2$  [3]. Thus, a U-shaped configuration [10] with close packing of hydrophobic tails can be proposed as the possible molecule structure in a monolayer at the surface of water (Fig. 4(a)).

Another possibility is an extended form of the molecule with strong inclination of the latter with respect to the water surface (Fig. 4(b)). We consider the last variant to be hardly probable. Indeed, in this case the tilt angle of the chain axes must be approximately  $60^\circ$  if the principle of close packing of the molecules [15] is valid. This value is obtained proceeding from the cross-section of two chains of  $0.54 \text{ nm}^2$  and the area per molecule, which should be a little more than  $1 \text{ nm}^2$ . An extended molecule in a non-compressed monolayer, or a slightly bent one with both hydrophilic groups immersed in water and hydrophobic chains pushed out from water owing to this small bend, must occupy initially an area of about  $5.0 \text{ nm}^2$  at the subphase surface. The last value can be estimated from the geometrical dimensions of the lipid [3]. When compressing the monolayer molecules will begin to interact at an area per molecule of  $5.0 \text{ nm}^2$  at least. The surface pressure should increase as the result. Taking into account these data one can expect for the molecules in an extended form a very sloping surface pressure–area isotherm with indistinctly expressed collapse.

Unlike this situation, the real surface pressure–area isotherm is very sharp, surface pressure is practically equal to zero up to  $1.1 \text{ nm}^2$ , and collapse pressure is well defined. Proceeding from these data one can suppose that initially, before compression, molecules are strongly bent, so that four chains are closely packed and the molecule occupies a small area.

Although close packing of the hydrophobic tails of the usual surfactant molecules in a monolayer is always advantageous because of their Van der Waals interaction, the possibility of formation of strongly bent archaeol molecules in a U-shape after spreading is not obvious. Two chains of the archaeol molecule are linked to the hydrophilic groups from both sides and this bend cannot occur in an arbitrary manner. Rough models of the bend caused by simultaneous rotation of the fragments of the chains around several single bonds can be proposed. However, such a possibility should be proved by detailed conformation analysis.

### 3.3. Structure of PH-GDGT molecules in LB films

Let us consider now what can happen during transfer of the monolayer composed of PH-GDGT molecules in a U-shape onto the substrate. The slope of the surface pressure–area isotherm at high pressure seems to be caused only by the compressibility of the condensed monolayer with a close packing of the chains. Indeed, the compressibility of the PH-GDGT monolayer evaluated from this slope at the pressure of deposition is only 2.5–4.5-times higher than that for monolayers of fatty acids and is practically equal to the compressibility of some fatty acid salts, in particular, that of barium stearate monolayer at  $\text{pH} \geq 8$  or zinc behenate monolayer at  $\text{pH} \geq 7$ . However, some increase of compressibility values for archaeol monolayers with respect to those of the usual surfactants can take place because the hydrophobic region in the first case is a complex mixture of isopranyl chains with different numbers of cyclopentane rings and their packing cannot be perfect. This is confirmed also by electron diffraction study. Deposited films are amorphous in a layer plane. If compressibility of the monolayer with closely packed molecules is the main cause of the slope of the surface pressure–area isotherm in the upper part, the area per molecule after deposition should correspond with satisfactory accuracy to that in a monolayer at the air–water interface extrapolated to zero surface pressure, i.e. about  $1 \text{ nm}^2$ . One can establish such a correspondence from electron diffraction data [16,17] for a number of surfactant compounds.

The period value in normal direction under Y-type deposition gives us a monolayer thickness of  $2.4 \text{ nm}$ . The length of the isopranyl chain alone is approximately  $4 \text{ nm}$  [3]. Two variants of monolayer deposition can take place if data on area per molecule and on monolayer thickness are taken into account. Either molecules in a U-shape are transferred onto the substrate as they exist in the monolayer at the air–water interface (Fig. 4(c)) or some very specific rearrangement occurs when the shape of the molecule changes, but the area per molecule remains exactly the same as before (Fig. 4(d)). The probability of such an event seems to be small, and a U-shape for the molecules is preferred after deposition as well. Another argument against the extended form of the molecules is that the surface of the film always remains hydrophobic after dipping up the substrate from water while the models in Fig. 4(b,d) should give a hydrophilic surface. Contact angle



measurements carried out after deposition confirm the model of the structure with closely packed isopranyl chains and with hydrophilic groups disposed far from the surface. These data are discussed below. Thus, the molecular structure in the deposited LB films seems to be unlike that of lamellar phases of bulk specimens.

### 3.4. Instability of PH-GDGT films in water

As was mentioned before, the deposited films of the PH-GDGT are unstable in aqueous solutions. Pieces of the film of quite different thicknesses begin to come away from the substrate and to transfer into water in a few minutes. For this reason, the films of PH-GDGT cannot be used as matrices for valinomycin dissolution and for creation of sensitive systems for potassium ions. Such a behaviour seems to be caused by the nature of lipid molecules from archaea which form in reality stable membranes surrounded by water solution, so that their hydrophilic surfaces must interact strongly with water to ensure this stability. Thus, when the film is immersed in water, molecules of the latter penetrate in hydrophilic regions of the multilayer and form hydrogen bondings with lipid molecules. Finally, the layer of water rises between hydrophilic surfaces of adjacent monolayers which results in film instability. Strong interaction of hydrophilic groups of lipid molecules with water can also cause difficulties for LB film deposition.

### 3.5. Deposition and study of MS-GDGT and DS-GDGT films

To improve the quality of film deposition we decided to synthesize other bipolar derivatives of the GDGT with hydrophilic heads containing carboxyl groups, i.e. MS-GDGT and DS-GDGT. We expected a considerable increase of the interaction energy of hydrophilic groups with each other due to salt formation with metal ions dissolved in water as in the case of fatty acid salts. In reality, it appears that highly uniform LB films of barium salts of these compounds can be deposited easily by the LB technique. Transmission IR spectra of the LB films deposited onto silicon substrates confirm salt formation. These spectra show the appearance of the absorption bands in the region of  $1425\text{--}1560\text{ cm}^{-1}$  which can be assigned to the symmetric and asymmetric stretching vibrations of  $\text{CO}_2^-$  anion, while spectra of pure compounds in KBr pellets contain only the bands in the  $\text{C=O}$  stretching region of carboxyl and ester groups ( $1715\text{--}1740\text{ cm}^{-1}$ ). The areas per molecule of  $1.45\text{ nm}^2$  and  $1.47\text{ nm}^2$  extrapolated to zero surface pressure (Fig. 2) and periods in the normal direction of  $4.40$  and  $3.97\text{ nm}$  (Table 1) for the MS-GDGT and DS-GDGT respectively give preference to a U-shape for the molecules as in the case of PH-GDGT. In addition, isopranyl chains must be tilted to the layer plane because values of area per molecule are considerably more than the total cross-section of four chains ( $1.08\text{ nm}^2$ ).

The discussion on the behaviour of PH-GDGT monolayers and on the structure of PH-GDGT molecules in the LB films is practically valid for the case of MS-GDGT and DS-GDGT also. However, the slope of the surface pressure–area isotherm for DS-GDGT cannot be explained only by the compressibility of condensed monolayer, which must be of the same order as that for PH-GDGT and MS-GDGT monolayers. Thus, one may expect that some specific reorientation of the DS-GDGT molecules during compression happens. A variant of such a reorientation is discussed below.

The reproducibility of the results on deposition is considerably better for the DS-GDGT. That is demonstrated by average transfer ratios measured during the deposition of the films for X-ray diffraction studies (Table 1). The morphology of the DS-GDGT film is shown in Fig. 3(b). The attractive property of these films is their stability in water solutions caused by strong interaction of adjacent molecules with bivalent barium ions.

### 3.6. Peculiarity of MS-GDGT film structure

X-ray small-angle diffraction studies show that crystalline order of MS-GDGT films in the normal direction is worse than that of DS-GDGT multilayers because intensities of the Bragg peaks for MS-GDGT films are considerably smaller and values of full-width at half-maximum (FWHM) are larger (Table 1). In addition, the presence of some second phase in the MS-GDGT film may be expected because the diffraction curve contains a smooth step in the region of  $2\theta = 1.15\text{--}1.30^\circ$ . It may correspond to a Bragg reflection with the spacing of  $7.23 \pm 0.44\text{ nm}$  although this is not clear enough. If one supposes that this step corresponds to a Bragg reflection, the period of  $4.4\text{ nm}$  determined from the other two distinct Bragg peaks cannot be related to the second order of the spacing of  $7.23\text{ nm}$ , obviously. In principle, some small fraction of the MS-GDGT with the extended shape of molecules may be responsible for the appearance of this reflection. However, hydrophilic groups situated on the surface should decrease contact angles with respect to those for DS-GDGT films. That is not observed in reality, as shown below. A small content of a phase like that determined in bulk specimens of native lipids is also possible. Unfortunately, such insufficient data based only on unfounded supposition about the origin of this step cannot give an exact answer.

### 3.7. Probable reorientation of DS-GDGT molecules during compression of the monolayer

A specific feature of the DS-GDGT surface pressure–area isotherm is the expanded shape (Fig. 2). The slope of the curve shows compressibility of the monolayer unusual for the condensed state. Deposition of high quality LB films is unlikely also for the monolayers with such a compressibility. The behaviour of DS-GDGT monolayers may be related to the change of molecule tilt during the compression process. The isotherm is located between the curves for MS-GDGT



Table 2

Advancing contact angles for LB films of archaeol lipids deposited by LB and horizontal lifting (hl) techniques onto hydrophobic silicon substrates

Lipid	Conditions of deposition	Number of monolayers	Contact angle (deg.)	
			water	hexadecane
PH-GDGT	optimum	10	91 <sup>a</sup>	7
	optimum	20	90 <sup>a</sup>	6
	optimum	38	88 <sup>a</sup>	7
MS-GDGT	optimum	10	95	
	optimum	20	97	
	optimum	60	97	
DS-GDGT	optimum	14	95	
	optimum	20	97	
	optimum	34	97	
	optimum	40	98	
	optimum	102	98	
	pH 8.0, LB	106	98	
	pH 9.0, LB	106	96	
	pH 10.0, LB	40	95	
	pH 10.0, LB	100	95	
	pH 2.0, hl	150	88 <sup>a</sup>	
	pH 3.1, hl	180	89 <sup>a</sup>	
	pH 4.6, hl	190	91 <sup>a</sup>	
	pH 5.6, hl	180	93	
	pH 6.6, hl	180	93	
	pH 7.4, hl	180	96	
	pH 8.5, hl	180	95	
	pH 9.0, hl	180	93	
	pH 10.0, hl	180	93	
	pH 11.0, hl	180	93	

<sup>a</sup> See explanations in the text.

and PH-GDGT. Thus, taking into account the usual compressibility of the monolayers of such lipids evaluated, for example, from the curves (a) and (b) in Fig. 2 we can expect that DS-GDGT molecules are tilted first to the layer plane like MS-GDGT molecules, and finally they are arranged like PH-GDGT molecules, i.e. with approximately vertical orientation of the chains. However, the real tilt of the chains in the deposited films as well as the real area per molecule are not known because it is not clear from what point and with which slope the surface pressure–area isotherm should be extrapolated to zero surface pressure. Substitution of the U-shape of DS-GDGT molecule by the extended one under compression seems to be impossible because both hydrophilic groups of the molecule are exactly the same and energies of their interaction with water are equal to each other. Such a possibility is also in strong contradiction with contact angle measurements carried out after deposition.

### 3.8. Contact angle measurements

Data on measurements of advancing contact angles for water for LB films of DS-GDGT, MS-GDGT, and PH-GDGT are shown in Table 2. Each value is an average of 4–6 meas-

urements in different places on the substrate. Contact angles for the films deposited under optimum conditions reported in experimental section were measured immediately after deposition, 1 day after and approximately 1 week after deposition. The results appear to be practically the same within experimental error. Thus, the surface of the films does not reorganize with time. Advancing contact angles for MS-GDGT and DS-GDGT films deposited under optimum conditions as well as for DS-GDGT films deposited at different pH values from 5.6 to 11.0 are determined with an accuracy of about 1.5–2°. There is a difficulty measuring contact angles for PH-GDGT films and for DS-GDGT ones deposited by the horizontal lifting technique at pH ≤ 4.6 when a droplet of water is used. The boundary of the droplet begins to move along the film surface practically immediately after touching and the contact angle changes. When the droplet is removed from the sample with a stream of compressed air one can observe an area with a changed interference colour in the shape of a ring. At the same time, in the place where the water droplet initially touches the surface the film is not destroyed. We can conclude that the film is transferred partly or completely onto the air–water interface when the boundary of the droplet moves along the surface. Such a behaviour is in agreement with the fact that deposition of PH-GDGT films by the LB technique is carried out with considerable difficulties because of the strong interaction of hydrophilic groups with water. The same reason results in the impossibility of DS-GDGT film deposition with the LB technique at pH lower than approximately 4.5–4.7. Thus, the values of contact angles presented in Table 2 for these two cases have been estimated quickly at the moment of surface touching. Real values are expected to be higher.

To obtain an additional confirmation that the surface of PH-GDGT films is highly hydrophobic advancing contact angles for hexadecane have been measured. These data are also shown in Table 2. Unfortunately, measurements of contact angles for hexadecane in the case of DS-GDGT and MS-GDGT films are impossible because hexadecane spread over the surface of the sample, destroying the film.

We shall analyse the data on contact angle measurements regarding the problem of structure selection from the models shown in Fig. 4(c,d). To do that we compare our data with those for different monolayers and LB films adopted by Ulman [14] from numerous original works.

Strictly speaking, the structure exactly corresponding to the model in Fig. 4(d) is impossible because closely packed adsorbed monolayers with hydrophilic surfaces show zero or at least small contact angles immediately after sample preparation. The process of hydrophilic surface reorganization is rather slow and a change of contact angle can be detected. Such results, for example, have been obtained for the monolayers of OH-(CH<sub>2</sub>)<sub>11</sub>-SH and OH-(CH<sub>2</sub>)<sub>21</sub>-SH on gold. It is not a case of studied films which possess stable hydrophobic surfaces.

However, the structure can correspond approximately to the model in Fig. 4(d). One hydrophilic group may be situ-



ated near the upper boundary of the film in such a manner that it is concealed by the nearest  $-\text{CH}_3$  and  $-\text{CH}_2-$  groups, which form a thin hydrophobic covering layer. In other words, the molecule can be bent in the region near the hydrophilic group while the chains possess a practically extended shape. The values of contact angles for this model depend on the packing of hydrophobic isopranyl tails and on the distance from the film surface to the nearest oxygen atoms of hydrophilic groups which may form hydrogen bondings with water molecules.

The water advancing contact angle for perfect surfaces exposing closely packed methyl groups is equal to  $111\text{--}115^\circ$ , while for the usual LB films of cadmium arachidate this value is less because of non-perfect packing of the molecules and equals  $106\text{--}110^\circ$ . On the other hand, for a smooth polyethylene surface exposing closely packed methylene groups the water contact angle is  $102\text{--}103^\circ$ , i.e. the difference of contact angles for ideal surfaces exposing closely packed methyl and methylene groups respectively is equal to  $9\text{--}12^\circ$ . Taking into account the fact that the hydrophobic region of the archaeol monolayer is a complex mixture of isopranyl chains of different structures [13], the ratio of the contents of methylene to methyl groups in this region can be estimated to be 67–75%. For rough calculations we can postulate that methylene and methyl groups will be exposed on the surface of the LB film with the same ratio and that a small decrease of contact angle with respect to the value of  $106\text{--}110^\circ$  is proportional to this ratio. In this case, the water contact angles for LB films of archaeol lipids composed of the molecules in a U-shape are expected to be of  $99\text{--}104^\circ$ . The same evaluations for the hexadecane contact angle give a value of  $10\text{--}13^\circ$ .

The experimental water contact angles for high quality DS-GDGT and MS-GDGT films deposited by the LB technique (Table 2) are under the evaluated lower limit by  $1\text{--}2^\circ$ . On the one hand, such a difference can take place because packing of the chains in archaeol LB films is worse than that in LB films composed of the usual amphiphilic molecules. On the other hand, it cannot be explained by the presence of oxygen atoms near the surface concealed by a thin hydrophobic layer of  $-\text{CH}_3$  and  $-\text{CH}_2-$  groups. Indeed, in the case of derivatized thiol monolayers on gold the water contact angle is equal to  $112^\circ$  for  $\text{HS}-(\text{CH}_2)_{21}-\text{CH}_3$  monolayers and decreases up to  $74^\circ$  and  $67^\circ$  for  $\text{HS}-(\text{CH}_2)_{11}-\text{O}-\text{CH}_3$  and  $\text{HS}-(\text{CH}_2)_{10}-\text{CO}_2-\text{CH}_3$ , respectively. Hydrophilic groups of the deposited archaeol lipids interact with water more strongly than simple ether and ester groups. Thus, in the case of archaeol multilayers with hydrophilic groups situated near the film surface the contact angle should decrease not less than by  $30\text{--}35^\circ$  with respect to the above evaluated value of  $99\text{--}104^\circ$ . Contact angles for the thiols with an ether linkage in different positions ( $\text{CH}_3-(\text{CH}_2)_n-\text{O}-(\text{CH}_2)_{10}-\text{SH}$ ) approach the value measured on a monolayer of  $\text{HS}-(\text{CH}_2)_{21}-\text{CH}_3$  if  $n$  is equal to 3. The same situation may take place in the LB films of archaeol lipids, i.e. the oxygen atoms of ether linkages should be situated at a distance of  $0.8\text{--}0.9$  nm at least from the film surface. However, this is already a

variant of the molecules in a U-shape although the exact position of the hydrophobic chain bend is indefinite.

The values of hexadecane contact angles for PH-GDGT films show that the film surface is more hydrophobic than the surface of polyethylene, for which the contact angle is  $0^\circ$ . Although the above predicted values are higher than the experimental ones, the difference can be also explained by insufficiently close packing of the molecules. In addition, we should take into account the possibility that the quality of PH-GDGT film deposition is not good enough, which may result in contact angle decrease.

Thus, data on contact angle measurements also show that a U-shape for the archaeol molecules in the LB films is preferred to an extended one.

Finally, from the data for DS-GDGT films deposited under different conditions (Table 2) we can conclude that packing of the molecules is better if the deposition is carried out by the LB technique. It seems that there is also an optimum pH range from 7 to 8 for close packing of the molecules. On the other hand, the quality of film deposition may be a reason for these small variations of contact angles as well. Indeed, optical microscopy observations show that more uniform LB films of DS-GDGT are deposited just by the LB technique at pH 7–8.

#### 4. Conclusion

LB films of native lipid extracted from thermophilic archaea have been deposited and studied, but the process of deposition is carried out with considerable difficulties. The films are unstable in water solutions. That seems to be caused by the chemical structure of hydrophilic groups which form numerous hydrogen bonds with water molecules. This interaction cannot be changed rationally by variation of water subphase composition.

The situation changes after chemical modifications of the native lipids. New synthesized compounds contain carboxyl groups in the hydrophilic heads. Interaction of the monolayers with each other becomes stronger due to salt formation with metal ions dissolved in the water subphase. As a result, the quality of deposition is considerably improved and the deposited films are not destroyed in aqueous solutions.

A U-shape for the molecules at the air–water interface and in the LB films is more probable than an extended one.

#### Acknowledgement

The present work was carried out within a contract relative to the National Program of Research on Bioelectronics, given by the Ministry of University and Scientific and Technological Research to Technobiochip Marciana (LI).



## References

- [1] O. Kandler, Where next with Archaeobacteria?, in M.J. Danson, D.W. Hough and G.C. Lunt (eds.), *Archaeobacteria: Biochemistry and Biotechnology*, Portland Press, London, 1992, pp. 195–207.
- [2] A. Gambacorta, A. Trincone, B. Nicolaus, L. Lama and M. De Rosa, *System. Appl. Microbiol.*, **16** (1994) 518.
- [3] A. Gulik, V. Luzzati, M. De Rosa and A. Gambacorta, *J. Mol. Biol.*, **182** (1985) 131.
- [4] A. Gulik, V. Luzzati, M. De Rosa and A. Gambacorta, *J. Mol. Biol.*, **201** (1988) 429.
- [5] K. Blodgett and I. Langmuir, *Phys. Rev.*, **51** (1937) 964.
- [6] G.G. Roberts, *Langmuir–Blodgett Films*, Plenum Press, New York, 1990.
- [7] H. Kuhn, *Thin Solid Films*, **99** (1983) 1.
- [8] Z. Kozarac, A. Dhathathreyan and D. Möbius, *FEBS Lett.*, **229** (1988) 372.
- [9] R. Rolandi, H. Schindler, M. De Rosa and A. Gambacorta, *Eur. Biophys. J.*, **14** (1986) 19.
- [10] M. Tomaia-Cotisel, E. Chifu, J. Zsako, A. Mocanu, P.J. Quinn and M. Kates, *Chem. Phys. Lipids*, **63** (1992) 131.
- [11] J.L. Dote, W.R. Barger, F. Behroozi, E.L. Chang, S.-L. Lo, C.E. Montague and M. Nagumo, *Langmuir*, **6** (1990) 1017.
- [12] M. De Rosa, A. Gambacorta and A. Gliozzi, *Microbiol. Rev.*, **50** (1986) 70.
- [13] M. De Rosa, A. Gambacorta, B. Nicolaus, B. Chappe and P. Albrecht, *Biochim. Biophys. Acta*, **753** (1983) 249.
- [14] A. Ulman, *An Introduction to Ultrathin Organic Films: From Langmuir–Blodgett to Self-assembly*, Academic Press, New York, 1991.
- [15] A.I. Kitaigorodskii, *Molecular Crystals and Molecules*, Academic Press, New York, 1973.
- [16] L.H. Germer and K.H. Storks, *J. Chem. Phys.*, **6** (1938) 280.
- [17] L.A. Feigin, Yu.M. Lvov and V.I. Troitsky, *Sov. Sci. Rev., Sec. A: Phys. Rev.*, **11**, part 4 (1989) 285.